Direct Concentration Approach of Moisture Diffusion and Whole-Field Vapor Pressure Modeling for Reflow Process—Part II: Application to 3D Ultrathin Stacked-Die Chip Scale Packages

B. Xie
Advanced Electronic Manufacturing Center,
School of Mechanical Engineering,
Shanghai Jiao Tong University,
Shanghai 200240, China

X. J. Fan[1]
Department of Mechanical Engineering,
Lamar University,
P.O. Box 10028,
Beaumont, TX 77710;
Department of Engineering Mechanics,
South China University of Technology,
Guangzhou 510640, China
e-mail: xuejun.fan@lamar.edu

X. Q. Shi
Hong Kong Applied Science and Technology
Research Institute,
2 Science Park East Avenue,
Shatin, Hong Kong

H. Ding
Advanced Electronic Manufacturing Center,
School of Mechanical Engineering,
Shanghai Jiao Tong University,
Shanghai 200240, China

*In the present study, the direct concentration approach (DCA) and the whole-field vapor pressure model developed in Part I of this work (Xie et al., 2009 "Direct Concentration Approach of Moisture Diffusion and Whole Field Vapor Pressure Modeling for Reflow Process: Part I–Theory and Numerical Implementation," ASME J. Electron. Packag., **131**, p. 031010) is applied to 3D ultrathin stacked-die chip scale packages to investigate wafer-level die-attach film cohesive failures during the reflow process. Oversaturation, which refers to the film that absorbs more moisture when reflow process begins, is observed using the DCA. The modeling results suggest that the moisture transport and escape through the substrate during the reflow is responsible for the film rupture. A small reduction in substrate thickness could result in a significant decrease in moisture concentration and vapor pressure in bottom layer film and therefore reduce failure rate greatly. A slight improvement in reflow profile while still meeting specification allows a significant amount of moisture loss during the reflow; hence failure rate could also be reduced greatly. The mechanism of soft film rupture at reflow due to moisture is discussed in detail. The simulation results are consistent with the published experimental data.* [DOI: 10.1115/1.3144154]

Keywords: direct concentration approach, moisture diffusion, vapor pressure, reflow, chip scale package, soft film, cavitation, unstable void growth, wafer level film (WLF), cohesive failure, die-attach, desorption

1 Introduction

The development of three-dimensional (3D) multidie stacking technology has become essential to increase functionality and memory capacity in more complex architectures and smaller-form factor packages. Wafer thinning is required to reduce die-thickness from original 750 μm to 50 μm or lower. Traditional dispense die-attach method with paste material is not capable of handling thinner dies. Wafer level films (WLFs) for die-to-die or die-to-substrate attachment were introduced in Refs. [1–6]. WLFs usually have a low glass transition temperature and substantially low Young's modulus (can be a few megapascals) at soldering reflow temperature. Figure 1 is a plot of storage modulus of a die-attach film with and without moisture [2,5]. It can be seen that the modulus decreases substantially when the temperature exceeds the glass transition temperature. As a consequence, film rupture may take place during the reflow process. Figure 2(*a*) is a through transmission scanning acoustic microscopy image of a 6×6 array stacked-die chip scale package (CSP) panel, showing massive failures inside packages (black regions) after the reflow. A cross-section view of a package confirms a large-scale cracking and voiding in the die-attach film attached to the substrate (called as the bottom layer film), as shown in Fig. 2(*b*). Other layers of films, which are sandwiched by dies, remain intact. Moisture is believed to be responsible for the failures. The bottom layer film absorbs moisture through the plastic substrate, while films in other layers absorb much less moisture. Therefore, no failures happen in other layers. It is noted that such a cohesive failure mode is different from the traditional interface delamination during the reflow, in which adhesion reduction due to moisture is the root cause [7–9].

Numerous designs of the experiment were executed for material screening and process optimization in developing stacked-die CSPs [2–5]. It has been found that package failure rates are very sensitive to substrate thickness and reflow profiles. Moisture uptake and transport during soldering reflow has been determined to be the root cause for these failures [2–5]. In the present study, the direct concentration approach (DCA) and the whole-field vapor pressure model developed in Part I of this work are applied to 3D ultrathin stacked-die CSPs. A simple bimaterial model, which represents a structure of the bottom layer film attached to a substrate, is analyzed first. Moisture redistribution, film "oversaturation," and vapor pressure evolution during the reflow are studied in detail with this model. Two scenarios of vapor pressure buildup at reflow are identified. The DCA and whole-field vapor pressure

[1]Corresponding author.

Contributed by the Electrical and Electronic Packaging Division of ASME for publication in the JOURNAL OF ELECTRONIC PACKAGING. Manuscript received September 18, 2008; final manuscript received March 22, 2009; published online July 31, 2009. Assoc. Editor: Cemal Basaran.

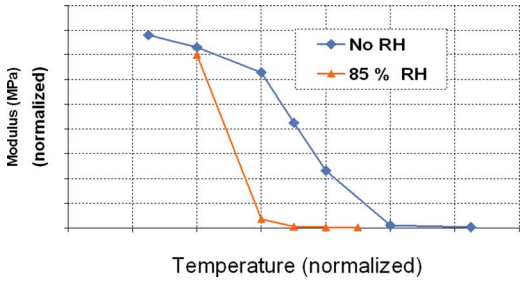

Fig. 1 Storage modulus of a die-attach film with and without moisture absorption as a function of temperature

analysis are then applied to ultrathin CSPs with different substrate thicknesses. The effect of reflow profiles is investigated. Failure mechanism of film rupture due to moisture is discussed.

2 Theory

Moisture concentration is discontinuous at the interface when two materials, which have different saturated moisture concentrations (C_{sat}), are joined together. Since commonly-used thermal-moisture analogy method cannot be applied to a reflow process [10], the DCA is used in the present study. In the DCA, the moisture concentration C is directly used as the basic field variable. In order to account for interfacial discontinuity, two separate sets of nodes are applied at a bimaterial interface to represent the discontinuity. Constraint equation is applied for each pair of nodes to satisfy the following continuity requirement:

$$\frac{C^{(1)}}{S(t)^1} = \frac{C^{(2)}}{S(t)^2} \tag{1}$$

where C^1 and C^2 are the moisture concentrations, and S^1 and S^2 are the solubilities of Mat1 and Mat2, respectively.

It is noted that the constraint equations must be updated each incremental time step [10]. Temperature and moisture fields are sequentially-coupled during the reflow process. In order to perform a fully coupled thermal-moisture analysis, additional field variable is defined. The vapor pressure can be calculated at each time step when moisture distribution solution is obtained. The vapor pressure model can be summarized with the following equations:

$$p(T) = \frac{RT}{\mathrm{MM}_{H_2O} f} \cdot C \quad \text{when} \quad C(T)/f < \rho_g(T) \tag{2a}$$

$$p(T) = p_g(T) \quad \text{when} \quad C(T)/f \geq \rho_g(T) \tag{2b}$$

where f is the free volume fraction, which is considered as an intrinsic material property, ρ_g is the saturated water vapor density, R is the universal gas constant (=8.314 J/(mol K)), MM_{H_2O} is the molecular mass of water (=18 g/mol) per mol, p_g is the saturated vapor pressure, and C is the moisture concentration from moisture diffusion analysis.

A user-defined FORTRAN subroutine is written for ABAQUS to compute for the vapor pressure and display the contour of vapor pressure at each time step.

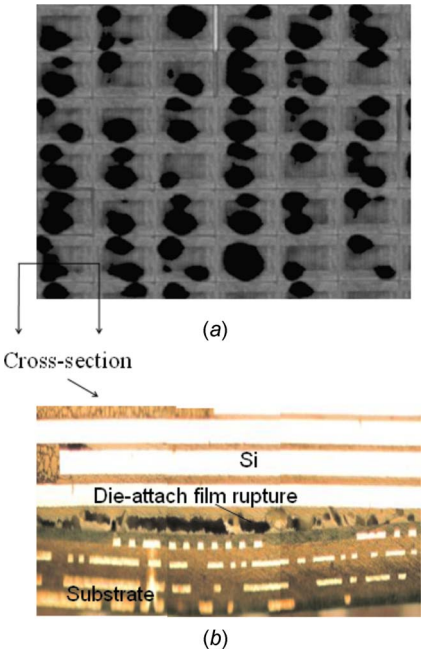

Fig. 2 (*a*) A TSAM image on a 6×6 array CSP panel (black regions mean failures inside packages) and (*b*) die-attach film cracking and voiding at the bottom layer attached to the substrate

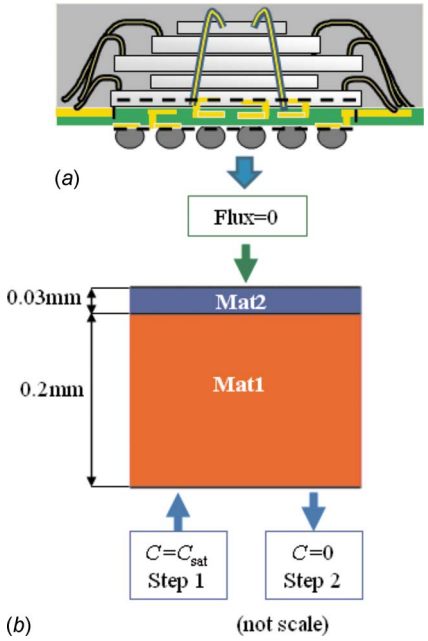

Fig. 3 (*a*) A schematic diagram of a stacked-die CSP and (*b*) a bimaterial model for moisture diffusion analysis (Mat1: substrate; Mat2: die-attach film)

3 A Bimaterial Model: Moisture Diffusion and Vapor Pressure Analysis

3.1 Moisture Diffusion. A schematic diagram of a stacked-die CSP is shown in Fig. 3(*a*). Since the distance from the package side to the die-attach film edge is greater than the substrate thickness, moisture in the bottom layer film is absorbed mainly through the substrate. Therefore, the problem can be simplified to a bimaterial model, as shown in Fig. 3(*b*). Mat1 represents the substrate and Mat2 represents the die-attach film, respectively. In order to further simplify the problem, a two-step loading is considered first. Step 1 is a constant temperature/humidity condition at 60°C/60% RH (for 88 h), followed by Step 2 with a step change to 260°C with zero RH. Tables 1 and 2 give the material properties at 60°C/60% RH and 260°C/60% RH, respectively. It is noted that the saturated moisture concentration for the die-attach (Mat2) at 260°C/60% RH is almost doubled that at

Table 1 Material properties at 60°C/60% RH

60°C/60% RH	Mat1	Mat2
Diffusivity D (mm^2/s)	1.28×10^{-5}	2.93×10^{-5}
C_{sat} (kg/m^3)	4.7	4.512
Solubility S (kg/m^3 Pa)	3.92×10^{-4}	3.76×10^{-4}

60°C/60% RH [11]. In the following, only the results in step 2 are shown (reflow process).

Figure 4 shows the results of moisture concentration in film and substrate at the interface as a function of time. It is observed that the moisture concentration in film has a "jump" in the beginning, while there is a drop in the substrate when desorption takes place. This is due to the new continuity requirement according to Eq. (1). It can be seen that the moisture concentration in film increases first, and then decreases with time. The local moisture gradient drives more moisture diffusing into the film in the beginning of the reflow process. Such a phenomenon is called oversaturation.

The distributions of moisture concentration in thickness direction at different times for Step 2 are plotted in Fig. 5. The moisture concentration at the boundary exterior is always zero. The moisture concentration is obviously discontinuous at the interface. In the beginning, the moisture concentration at the interface is redistributed according to the new continuity requirement. The redistribution causes moisture in the substrate at the interface less than in the bulk and moisture in the film at the interface greater than in the film bulk. Such a local moisture gradient will drive more moisture diffusing into the die-attach film from the substrate despite that an overall desorption process goes on. After a certain time (e.g., 20 s), moisture in the film eventually starts to decrease. It is noted that the total amount of moisture content at the interface, in the beginning, does not change much since the diffusion is not fast enough to change the total amount of moisture at the interface.

3.2 Vapor Pressure Analysis. In order to capture accurately the vapor pressure buildup during the reflow, a real reflow loading profile is applied here instead of using a step function in the preceding analysis. Figure 6 gives two reflow profiles that will be used in the subsequent analysis. Profile 1 in Fig. 6 is applied here. Several incremental steps are divided to simulate such an actual

Table 2 Material properties at 200°C/60% RH

200°C/60% RH	Mat1	Mat2
Diffusivity D (mm^2/s)	4.72×10^{-4}	6.43×10^{-4}
C_{sat} (kg/m^3)	4.7	9.024
Solubility S (kg/m^3 Pa)	5.05×10^{-6}	9.7×10^{-6}

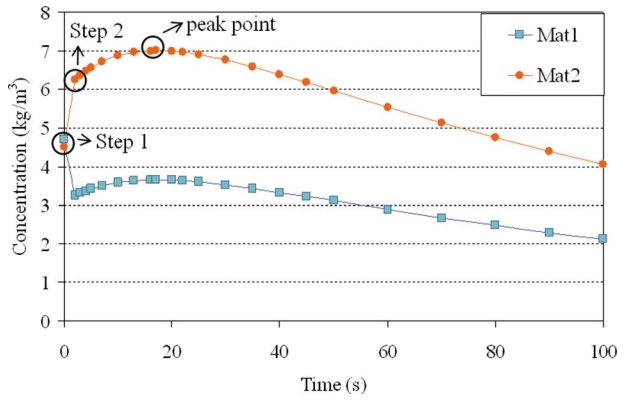

Fig. 4 Moisture diffusion history plot at the interface in Step 2

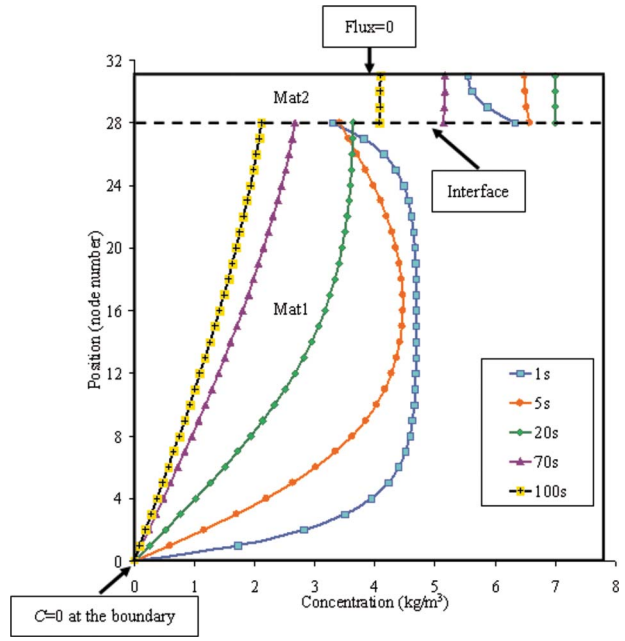

Fig. 5 Moisture concentration distributions in Step 2

profile. The free volume fraction f is assumed to be 0.05 [11,12]. Figure 7 plots the vapor pressure and moisture concentration in the die-attach during the reflow. Results show that the vapor pressure increases exponentially and coincides with the saturated water vapor pressure curve. This implies that the moisture is in the mixed liquid/vapor state, according to Eq. (2). Around 220°C, the vapor pressure reaches a peak value (about 3 MPa) and then starts to decrease gradually even though the temperature continues to

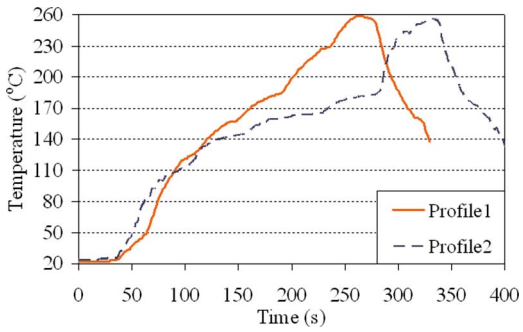

Fig. 6 Two reflow loading profiles used in the present study

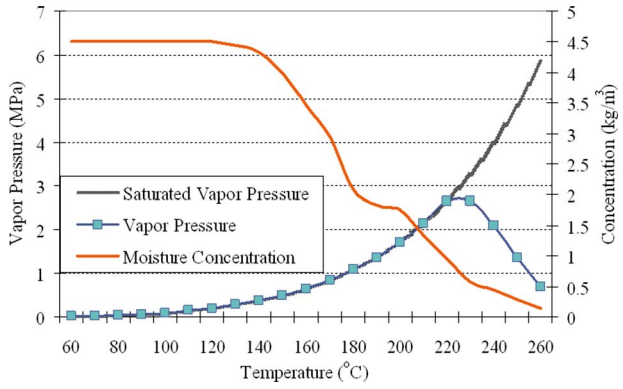

Fig. 7 History plots of vapor pressure and moisture concentration at the interface during the reflow

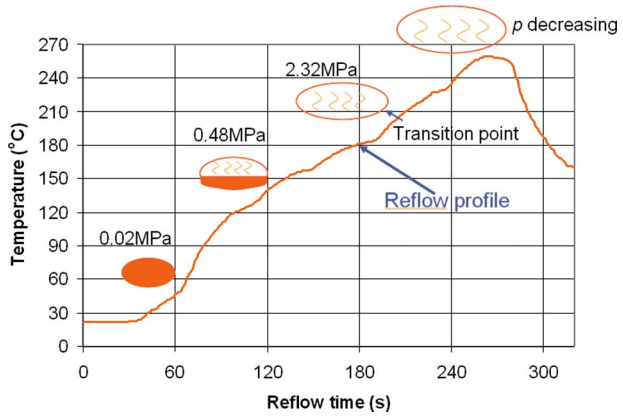

Fig. 8 Schematic diagram for Scenario I of vapor pressure buildup during the reflow

increase. This is because moisture diffuses out of the package during the reflow. When there is no sufficient residual moisture remaining in the film to keep it as a binary state, the vapor pressure will decrease.

Two scenarios of vapor pressure buildup during the reflow have been identified [2], as shown in Figs. 8 and 9, respectively. Before the reflow process starts, moisture condenses in nanopores or free volumes. With increasing temperature, more and more moisture will be vaporized. At the same time, the moisture concentration will decrease as more and more moisture will be diffused out of the package. At a certain point (temperature), the moisture may become fully vaporized. This point is a transition temperature for moisture from a binary state to a single vapor state. When the temperature further increases, moisture is lost further. Therefore, the vapor pressure will drop, as shown in Fig. 8. This is referred to as Scenario I of the vapor pressure buildup. Film rupture may not occur if the peak pressure is less than the critical stress of the material. Scenario II refers to the case in which moisture in free volumes is always in a binary liquid/vapor state, as shown in Fig. 9. In this case, the vapor pressure will be the same as the saturated water vapor pressure. If the vapor pressure reaches the critical stress of the material, rupture will take place. Although the difference in magnitude of the vapor pressure between these two scenarios is very narrow (less than a few megapascals), such a narrow difference will make dramatic difference in the reflow performance [2,5].

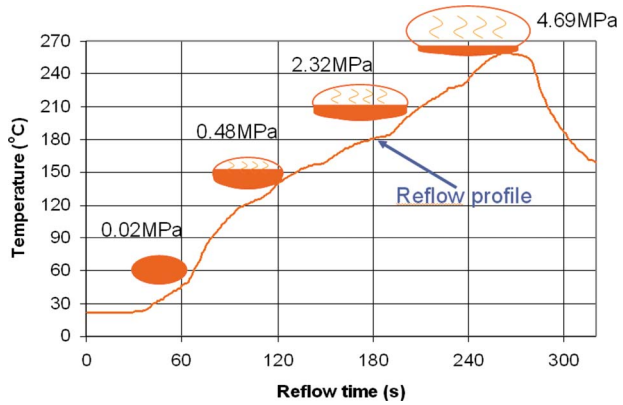

Fig. 9 Schematic diagram for Scenario II of vapor pressure buildup during the reflow

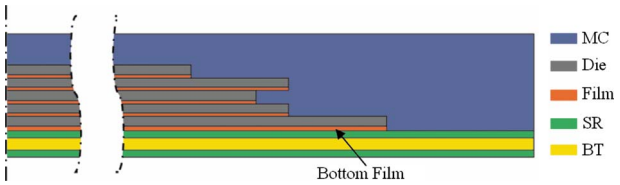

Fig. 10 Schematic structure of a 3D ultrathin stacked-die chip scale package

4 Application to 3D Ultrathin Stacked-Die Chip Scale Packages

Vapor pressure development during the reflow is closely related to moisture concentration distributions; thus it becomes essential to accurately simulate moisture diffusion during a reflow process. Finite element analysis for a 3D ultrathin stacked-die chip scale package is conducted. The package is composed of the mold compound (MC), multiple silicon dies, multiple die-attach films, solder resist (SR), and BT core, as shown in Fig. 10. The substrate includes two layers of SR and one layer of BT. In the following study, packages are applied to a moisture preconditioning at 60°C/60% RH for 88 h, followed by a reflow process. Two reflow profiles, shown in Fig. 6, will be applied. It was shown that moisture soaking at 60°C/60% RH for 88 h is equivalent to the JEDEC moisture sensitivity level 3 (MSL3) condition [13].

4.1 Effect of Substrate Thickness. Two substrate thicknesses of 200 μm and 280 μm [14] are simulated with Reflow Profile 1. Results for both moisture concentration and vapor pressure in film were obtained. Figure 11 shows the contours of moisture concentration at 260°C for packages with different substrate thicknesses. For thinner substrate, the moisture concentration in the bottom layer film is 54% less than in the thicker substrate. It is also observed that there is virtually no difference in the moisture concentration in the MC and other films. Significant moisture in the bottom layer film is lost through the substrate during the reflow. This indicates that substrate thickness plays a key role in thin package moisture performance.

Figure 12 shows the history of local moisture concentration in the bottom layer film for two substrate thicknesses. It can be seen that the difference in moisture concentration becomes significant when the temperature is above 150°C. Such a difference tends to be small again when the temperature is beyond 250°C since both packages tend to be dried out eventually with time.

The contours of vapor pressure are shown in Fig. 13 for two substrate thicknesses. For the thinner substrate, the vapor pressure is 40% less than in the thicker substrate. Figure 14 shows the histories of vapor pressure evolution for these two cases. The package with the thinner substrate follows Scenario I of vapor pressure buildup with a pressure drop, while the package with the thicker substrate follows Scenario II, in which the vapor pressure

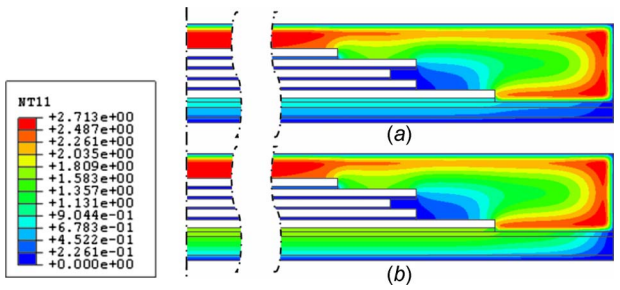

Fig. 11 Moisture concentration contours of a CSP at 260°C using the DCA: (*a*) a thinner substrate and (*b*) a thicker substrate

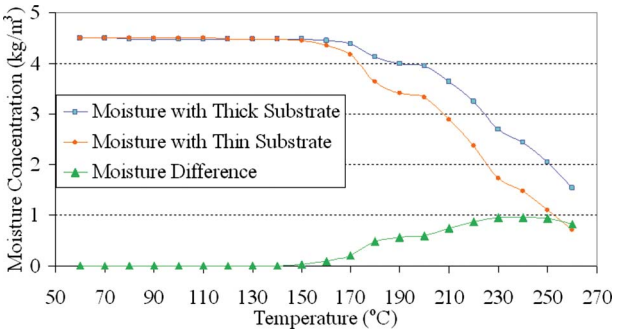

Fig. 12 Moisture concentration comparison between two substrate thicknesses

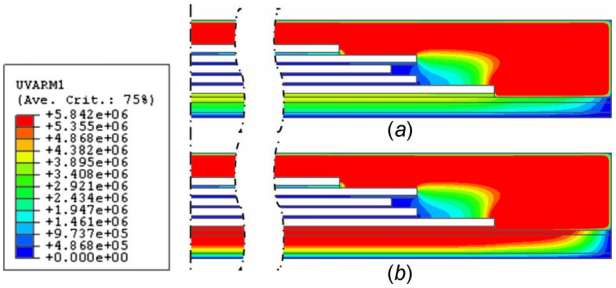

Fig. 13 Vapor pressure contours of a CSP at 250°C: (*a*) a thinner substrate and (*b*) a thicker substrate

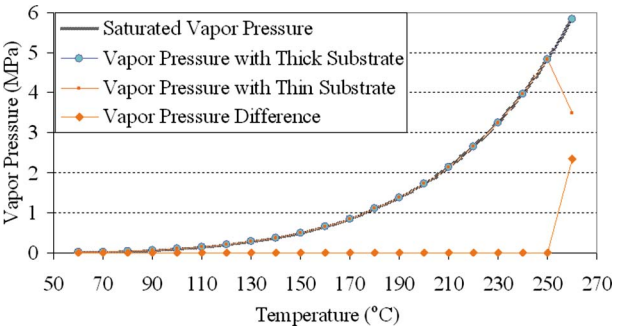

Fig. 14 Vapor pressure comparison between two substrate thicknesses

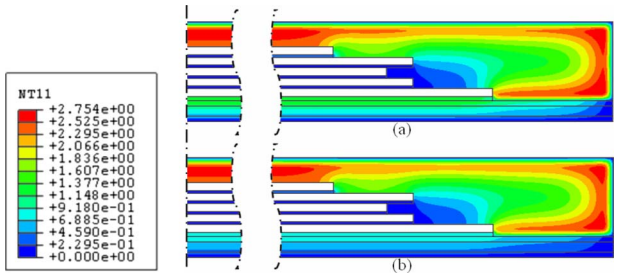

Fig. 15 Moisture concentration contours at 250°C subjected to two different reflow profiles

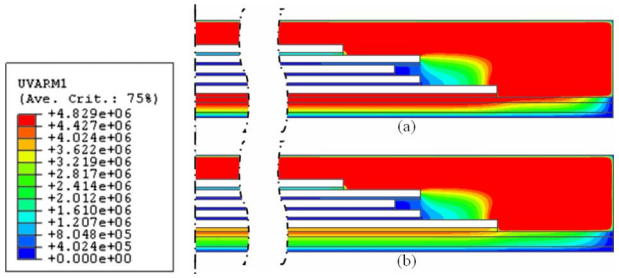

Fig. 16 Vapor pressure contours at 250°C subjected to two different reflow profiles

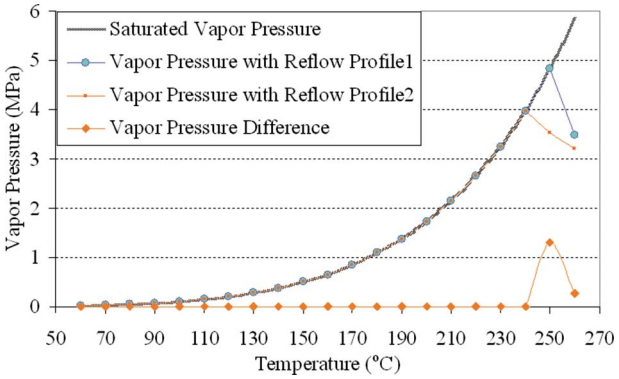

Fig. 17 Vapor pressure comparison between two substrates

remains saturated at 260°C. Experimental results [4] showed that the failure rate for the thicker substrate is much higher for the thinner substrate, which are consistent with the DCA predictions.

4.2 Effect of Reflow Profile. Two different reflow profiles shown in Fig. 6 are applied here. These two profiles satisfy the JEDEC standard specification on temperature ramp up as a function of time. The main difference in these two profiles is that Profile 2 has an extended time period (approximately about 90 s) before the temperature ramps up rapidly to the peak temperature from a temperature of 150°C, compared to the Reflow Profile 1. Both profiles have the same peak temperature of 260°C.

The package, with a substrate thickness of 280 μm, is used here to study the effect of the reflow profile. Figure 15 plots the contours of moisture concentration at 250°C for these two reflows. When Reflow Profile 2 is applied, the moisture concentration in the bottom layer film is 34% less than with Reflow Profile 1. This is because Reflow Profile 2 has a longer exposure time at a level of temperature of 150°C to allow more moisture to be released before it ramps up. Figure 16 plots the contours of vapor pressure at 250°C subjected to the two profiles, respectively. For Profile 2, the vapor pressure in the bottom layer film is 27% less than with Profile 1.

Figure 17 plots the vapor pressure evolution in the bottom layer film. It can be seen that the vapor pressure buildup under Profile 2 follows Scenario I with a vapor pressure drop at the temperature of 240°C, while the vapor pressure under Profile 1 follows Scenario II with a saturated water vapor pressure. These results are consistent with the experimental observations [5].

5 Discussions

In the preceding analysis, thermal stresses are not taken into considerations. Vapor pressure is presumed to be a dominant driving force for film rupture. Since the film modulus at the reflow temperature is extremely low (only a few megapascals), thermal stress is orders lower than the modulus. Even the finite-deformation theory is applied, the critical void volume fraction for the material to collapse is relatively small [15–17]. This implies that thermal stress is a small fraction of the peak vapor pressure.

Huang et al. [3] performed finite element analysis and showed that thermal stress is in a compressive state at the reflow since the film expansion is constrained by surrounding materials with relatively higher stiffness.

From the experimental data and vapor pressure analysis, the critical stress for film to rupture is in a very narrow range, say, between 2 MPa and 6 MPa (a very rough estimate). A finite single spherical void model was introduced previously by one of the authors [1,15,16]. When the hyperelastic model is applied for a rubbery material, a nonlinear and nonmonotonic relationship between vapor pressure and void volume fraction is obtained within the context of finite-deformation theory. This defines a critical stress for the occurrence of unstable void growth. The critical stress is found to be in the same order of Young's modulus of the film when initial void volume fraction is between 0.01 and 0.05 [15,16]. Although a single finite spherical void model is too simple, it shed light on the mechanism of unstable void growth within the context of finite-deformation. It is also observed that such a film failure is caused by a hydrostatic stress. Huang et al. [3] introduced Gent and Lindley's [17] solution for a single spherical void in an infinite medium to explain the cavitation in a rubbery material and concluded that the failure is modulated by the modulus and surface energy of the material, as well as the initial void size.

Cohesive film failures at the reflow have not been observed previously when the dispense die-attach assembly method is applied [7–9,18,19]. A die-attach paste material has a much higher modulus than a wafer-level die-attach film. A reasonable estimate of Young's modulus for a die-attach paste material is at least 100 MPa at the reflow temperature [1]. In this case, according to the analysis from a single void model, cohesive rupture is not a concern, rather it is an interfacial delamination. Most of the previous studies focused on the interfacial delamination [7–9,18,19]. Another unique characteristic, for the ultrathin CSP package, is moisture desorption during the reflow process. Moisture loss along the substrate/film interface becomes significant during the reflow. However, for a regular type package, significant moisture is lost only in the exterior of the package.

6 Conclusions

When above glass transition temperature, the saturated moisture concentration of the die-attach film increases. As a result, the film absorbs more moisture when the reflow process begins despite that an overall desorption goes on. This is referred to as oversaturation. Oversaturation cannot last since moisture will be diffused out of the package eventually with time. Two scenarios of vapor pressure buildup were identified. Scenario I refers to a vapor pressure drop at a certain temperature during the reflow process, while Scenario II refers to a saturated water vapor pressure evolution all the time. Numerical results using the DCA confirm that the moisture concentration in the bottom film is significantly lower for a thinner substrate CSP than a thicker one. In addition, the vapor pressures in the film using the whole-field analysis show that the substrate thickness plays a key role in affecting the magnitude of the vapor pressure. Reflow profiles affect package moisture performance greatly. A slight improvement in the reflow profile, while still meeting JEDEC standard specification, allows a significant amount of moisture loss during the reflow; hence failure rate could also be reduced significantly. Simulation results on moisture concentration and vapor pressure are consistent with the published experimental data.

Acknowledgment

The authors would like to acknowledge the work and discussions with the moisture-induced failure focus team (MIFFT) members at Intel from sites in Chandler, AZ and Shanghai, China.

References

[1] Fan, X. J., 2005, 2006, 2007, 2008, "Moisture Related Reliability in Electronic Packaging," ECTC Professional Development Course Notes.
[2] Fan, X. J., Bekar, I., Fischer, A. A., He, Y., Huang, Z., and Prack, E., 2006, "Delamination/Cracking Root Cause Mechanisms for Ultra-Thin Stacked Die Chip Scale Packages," *Intel Conference on Manufacturing Excellence (IMEC)*, San Diego, CA.
[3] Huang, Z., Tang, J., Hu, C., Wang, M., Zhang, M., Liu, B., Fan, X. J., and Prack, E., 2006, "Moisture Induced Cohesive Delamination in Die-Attach Film in Ultra Thin Stacked Chip-Scale Package," Intel Assembly Test Tech, Journal.
[4] Prack, E., and Fan, X. J., 2006, "Root Cause Mechanisms for Delamination/Cracking in Stack-Die Chip Scale Packages," *IEEE International Symposium on Semiconductor Manufacturing (ISSM)*, pp. 219–222.
[5] Shi, X. Q., and Fan, X. J., 2007, "Wafer-Level Film Selection for Stacked-Die Chip Scale Packages," *Proceedings of the 57th Electronic Components and Technology Conference (ECTC)*, pp. 1731–1736.
[6] Xie, B., Shi, X. Q., and Fan, X. J., 2007, "Sensitivity Investigation of Substrate Thickness and Reflow Profile on Wafer Level Film Failures in 3D Chip Scale Packages by Finite Element Modeling," *Proceedings of the 57th Electronic Components and Technology Conference (ECTC)*, pp. 242–248.
[7] Fan, X. J., Zhang, G. Q., van Driel, W. D., and Ernst, L. J., 2008, "Interfacial Delamination Mechanisms During Soldering Reflow With Moisture Preconditioning," IEEE Trans. Compon. Packag. Technol., **31**(2), pp. 252–259.
[8] Zhang, G. Q., Driel, W. D. V., and Fan, X. J., 2006, *Mechanics of Microelectronics*, Springer, New York.
[9] van Driel, W. D., van Gils, M. A. J., Fan, X. J., Zhang, G. Q., and Ernst, L. J., 2008, "Driving Mechanisms of Delamination Related Reliability Problems in Exposed Pad Packages," IEEE Trans. Compon. Packag. Technol., **31**(2), pp. 260–268.
[10] Xie, B., Fan, X. J., Shi, X. Q., and Han, D., 2009, "Direct Concentration Approach of Moisture Diffusion and Whole Field Vapor Pressure Modeling for Reflow Process: Part I–Theory and Numerical Implementation," ASME J. Electron. Packag., **131**, p. 031010.
[11] Fan, X. J., Lee, S. W. R., and Han, Q., "Experimental Investigations and Model Study of Moisture Behaviors in Polymers," Microelectron. Reliab., to be published.
[12] Fan, X. J., Zhou, J., Zhang, G. Q., and Ernst, L. J., 2005, "A Micromechanics Based Vapor Pressure Model in Electronic Packages," ASME J. Electron. Packag., **127**(3), pp. 262–267.
[13] Shi, X. Q., Fan, X. J., and Xie, B., 2008, "A New Method for Equivalent Acceleration of JEDEC Moisture Sensitivity Levels," *Proceedings of the Electronic Components and Technology Conference (ECTC)*, pp. 907–912.
[14] He, Y., and Fan, X. J., 2007, "In-Situ Characterization of Moisture Absorption and Desorption in a Thin BT Core Substrate," *Proceedings of the Electronic Components and Technology Conference*, pp. 1375–1383.
[15] Fan, X. J., Zhang, G. Q., van Driel, W. D., and Ernst, L. J., 2003, "Analytical Solution for Moisture-Induced Interface Delamination in Electronic Packaging," *Proceedings of the Electronic Components and Technology Conference*, pp. 733–738.
[16] Fan, X. J., Zhang, G. Q., and Ernst, L. J., 2002, "A Micro-Mechanics Approach in Polymeric Material Failures in Microelectronic Packaging," *Proceedings of the Third International Conference on Thermal and Mechanical Simulation in Micro-Electronics (EuroSimE)*, pp. 154–164.
[17] Gent, A. N., and Lindley, P. B., 1959, "Internal Rupture of Bonded Rubber Cylinders in Tension," Proc. R. Soc. London, Ser. A, **249**(1257), 195–205.
[18] Fan, X. J., and Zhang, G. Q., 2002. Multi-Physics Modeling in Virtual Prototyping of Electronic Packages, *Proceedings of the Third International Conference on Thermal and Mechanical Simulation in Micro-Electronics (EuroSimE)*, pp. 29–37.
[19] Fan, X. J., Zhou, J., and Chandra, A., 2008, "Package Structural Integrity Analysis Considering Moisture," *Proceedings of the Electronic Components and Technology Conference (ECTC)*, pp. 1054–1066.